3rd Specialty Conference on Disaster Prevention and Mitigation
3e Conférence spécialisée sur la prévention et la mitigation des désastres naturels

Montréal, Québec
May 29 to June 1, 2013 / *29 mai au 1 juin 2013*

Investigation of the Shear Behaviour of Unbonded Fiber Reinforced Elastomeric Isolators (FREIs) with Modified Support Geometry

N. C. Van Engelen, D. Konstantinidis, M. Tait
Department of Civil Engineering, McMaster University

Abstract: The use of fiber reinforcement in lieu of traditional steel reinforcement for elastomeric seismic isolators has the potential for widespread application in developed and developing countries. If mechanical fasteners are not used when installing a Fiber Reinforced Elastomeric Isolator (FREI) between the supports, a unique roll-over deformation will occur when displaced horizontally. This roll-over deformation is a consequence of the lack of flexural rigidity of the fiber reinforcement and the unbonded application of the isolator. Unbonded FREIs have a non-linear shear relationship due to the roll-over behaviour. The non-linear relationship is a desirable feature as it allows the response of the isolator to be tailored depending on the horizontal force. Methods of predicting and modelling the non-linear relationship range from simplified analytical equations to complex finite element analysis. Three analytical models are reviewed and compared, outlining the fundamental assumptions and implications of each model. Shear relationships are compared against experimental results for two unbonded FREIs from the literature. Of the three models considered, only one provides an estimate of the deformed shape of the roll-over. This model is adapted to show the influence of modifications to the support geometry that can be used as an additional design parameter. Recommendations are made based on model results and areas requiring further investigation are identified and discussed.

1. Introduction

Economic losses from earthquakes in 2011 were the highest ever recorded worldwide at more than USD 226 billion in addition to the tragic loss of thousands of lives (Swiss Re 2012). This catastrophic impact is in part due to the unfortunate harmony that exists between the fundamental frequency of structures, especially low rise structures, and the high energy frequency range of a typical earthquake. The primary objective of modern design codes, such as the National Building Code of Canada, is to prevent the structural collapse. While it is estimated that more than 80 % of the value of an average office building is attributed to the contents and non-structural components, 90 % for an average hospital, these items are often overlooked (Taghavi and Miranda 2003). There is a high risk that damage will occur to a structure and its contents in large earthquake events despite modern construction methods.

A method of protecting the structure and the non-structural components and contents from earthquakes is to introduce a horizontally flexible layer at the foundation level. This process, known as base isolation, decouples the structure from the ground motions allowing large displacements to occur at the isolation layer. The isolation layer dominates the response, effectively shifting the fundamental frequency of the structure out of the critical high energy range. The structure translates on top of the isolation layer as a near-rigid block as shown in Figure 1, minimizing damage to the structure and its contents after large earthquake events.

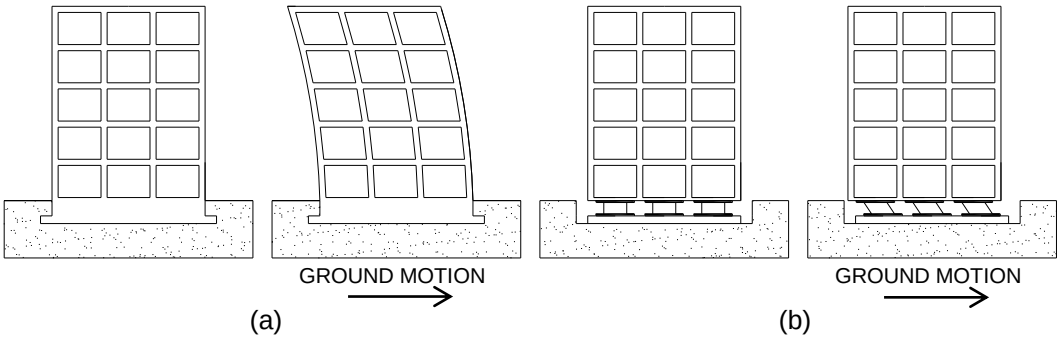

Figure 1: Idealized Response of a (a) Conventional Fixed Base Structure and a (b) Base Isolated Structure to Ground Motion

Elastomers are an ideal engineering material for application in base isolation due to their near incompressibility and low shear modulus. Conventional Steel Reinforced Elastomeric Isolators (SREIs) are heavy and expensive (Kelly and Marsico 2010). This has stood as a barrier to their widespread application, especially in developing countries where devastation due to earthquakes is often more severe. The significant weight of SREIs originates from the steel reinforcement and large steel end plates used to mechanically fasten the isolator to the supports. The cost originates in part from the manufacturing process required to bond the elastomer to the steel in order to resist the high tensile stresses that develop during horizontal displacement. As a means of alleviating these barriers, it has been proposed that the steel reinforcement be replaced with a lighter fiber reinforcement of similar mechanical properties in tension (Kelly 1999). Fiber Reinforced Elastomeric Isolators (FREIs) have been shown to perform similar to, or superior to, conventional SREIs of similar design (Moon et al. 2002).

The installation of FREIs can be further simplified by removing the large steel end plates used to mechanically fasten the isolator to the supports; utilizing the isolator in an unbonded application. Unbonded FREIs undergo a unique deformation shown in Figure 2. As the isolator is displaced horizontally, the corners of the isolator, initially in contact with the supports, lose contact. This process is known as *roll-over*. The roll-over deformation is a consequence of the lack of flexural rigidity of the fiber reinforcement and the unbonded application and is considered a desirable characteristic. The otherwise linear shear behaviour is complicated by the roll-over, creating a softening response as the amount of roll-over increases. The softening response is advantageous since it results in a larger shift of the fundamental frequency, increasing the efficiency of the isolator. Methods of modelling the shear relationship range from simplified analytical models to complex finite element analysis.

This paper presents and compares three analytical models. The shear relationships from the models are evaluated against experimental results. A model is used to investigate modified support geometry, which alters the roll-over performance of the isolator. The performance of each model is evaluated and areas requiring further investigation are identified and discussed.

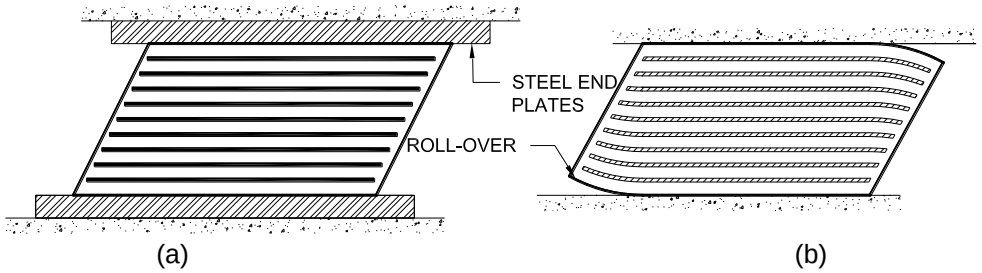

Figure 2: Deformed (a) Bonded Isolator with Rigid Reinforcement and (b) Unbonded Isolator with Flexible Reinforcement

2. Background

2.1 Initial Horizontal Displacement

It is convenient to analyze an unbonded FREI by dividing it into three sections based on the deformed shape at a horizontal displacement, *s* (Peng et al. 2009, Konstantinidis et al. 2008). The size and geometry of the three sections are a function of the horizontal displacement. The dimensions of the isolator are 2*a*, 2*b*, and *h* for the width, length, and total height, respectively. The initial width of the isolator is reduced by the horizontal displacement as roll-over occurs. The two identical roll-over sections are located on either side of the central section, as indicated in Figure 3. The vertical line, drawn from where the isolator loses contact with the supports to the opposite corner, indicates the division between the roll-over sections and the central section. The total horizontal force, *F*, can be expressed as the sum of the forces of the individual sections:

[1] $F = F_1 + 2F_2$

where F_1 is the contribution from the central section and F_2 is the contribution from a roll-over section.

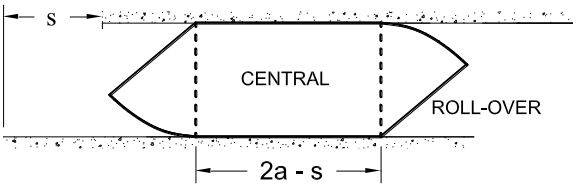

Figure 3: Division of an Unbonded FREI into Sections at a Horizontal Displacement, *s*

The central section of the isolator undergoes pure shear. The shear strain is assumed to be limited to the elastomeric layers with no strain occurring in the reinforcement. Thus, the force contribution from the central section can be expressed as:

[2] $F_1 = G_e \gamma A_r = G_e(s/t_r)(2b)(2a-s)$

where G_e is the shear modulus of the elastomer, $\gamma = s/t_r$ is the shear strain, t_r is the total thickness of the elastomeric layers and $A_r = 2b(2a-s)$ is the reduced loaded area. Equation 2 represents a lower-bound solution proposed by Konstantinidis et al. (2008). This solution is obtained by assuming that the roll-over sections are stress free and provide no contribution to the horizontal force such that $F_2 = 0$. Although γ is increasing, A_r is decreasing, which causes the force contribution from the central section to reach a maximum. At this point the isolator is prone to instability as the tangential horizontal stiffness becomes negative. This lower-bound solution is hereinafter referred to as Model 1.

There are two proposed approaches for determining the contribution of the roll-over sections. Both approaches assume the displacement of the roll-over section is due to contributions from shear and bending displacements, d_s and d_b, respectively. The shear displacement occurs over half the roll-over area of the free surface and thus is a function of *s*. An important distinction between Model 2, as proposed by Peng et al. (2009) and Model 3, a modified version of the model by Peng et al. (2009), is a consequence of the interpretation of the relationship between the roll-over section and horizontal displacement, which also alters the interpretation of the bending displacement. In Model 2, the horizontal displacement is assumed to equal the horizontal distance from the division of the section to the free corner of the roll-over section as shown in Figure 4a. In Model 3, it is assumed that the free surface of the roll-over is stress free. Therefore, the length of the free surface of the roll-over sections is equal to the horizontal displacement (Kelly and Konstantinidis 2007, 2011) as shown in Figure 4b.

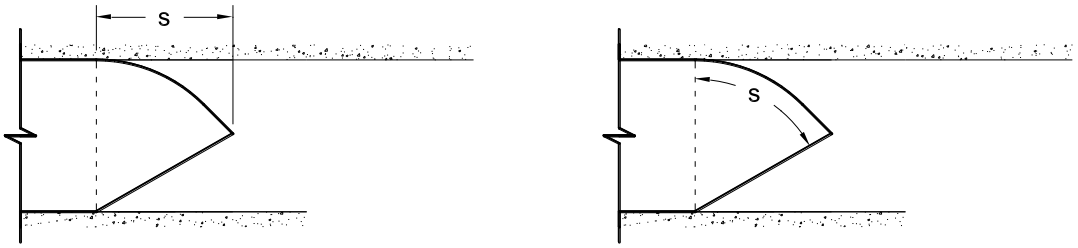

Figure 4: Roll-over Horizontal Displacement Relationships for (a) Model 2 and (b) Model 3

The roll-over section is viewed as a cantilever with an equivalent vertical point load. Based on the rotation, θ, as defined in Peng et al. (2009), the vertical point load can be related to the force contribution from the roll-over section. The vertical point load is equal to the sum of the individual contributions of each layer of elastomer and reinforcement which, due to the low shear modulus of the elastomer in comparison to the reinforcement, are assumed to act independently and not as a composite section. According to the displacement relationships and load assumptions, the governing relationship between s and θ for Model 2 is given by:

$$[3] \qquad \frac{2B\theta \tan\theta}{G_e\gamma^3} + h\sin\theta - s\sqrt{1-\frac{4\theta^2}{9}} = 0$$

and for Model 3:

$$[4] \qquad \frac{2B\theta \tan\theta}{G_e\gamma^3} + h\theta - s = 0$$

The parameter B is a constant based on the geometry of the isolator and is a function of the elastic modulus and thickness of each layer of elastomer and fiber reinforcement. The bending rigidity of the fiber reinforcement is assumed to be negligible in Model 3. Model 2 does not make this distinction. With s and θ determined the horizontal force contributions for each section can be calculated.

2.2 Full Roll-over

The amount of roll-over will continue to increase until the initially vertical faces of the isolator become horizontal and contact the upper and lower supports in opposite corners, denoted as *full roll-over,* illustrated in Figure 5. Only Model 3 considers the occurrence of full roll-over and the full roll-over performance. In a study conducted by Toopchi-Nezhad et al. (2008) it was indicated that unbonded FREIs have desirable characteristics after full roll-over occurs if stability is maintained. Full roll-over restrains the isolator from additional roll-over, resulting in a significant stiffening that is desirable to protect the structure against extreme displacements that may occur during beyond design basis events. Full roll-over performance is an important component of a comprehensive analytical model for unbonded FREIs.

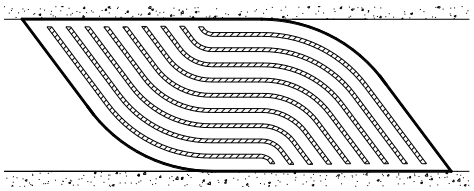

Figure 5: Full Roll-over of an Unbonded FREI

Model 3 predicts the occurrence of full roll-over by determining the deformed shape of the isolator as a function of d_s and d_b. By modelling the deformed shape of the roll-over section, the vertical, d_v, and

horizontal, d_h, displacement of the free corner, as shown in Figure 6, can be determined. Full roll-over is defined to occur when the magnitude of d_v is equal to h. Since continued roll-over is now constrained by the supports, the isolator, according to Model 3, reverts back to pure shear deformation. The division of the isolator previously defined remains unaltered; however a new force contribution, F_3, is included to account for the full roll-over behaviour of the roll-over sections. As additional roll-over is restricted, the area of the central section, A_r, is now constant. The force required to cause full roll-over, F_2, remains constant, and the additional force contribution, F_3, is a function of an effective shear area for the roll-over sections. The total force contribution can be expressed as:

[5] $$F = F_1 + 2F_2 + 2F_3$$

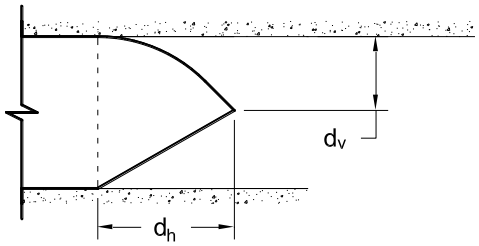

Figure 6: Model 3 Deformed Shape of the Roll-over Section and Position of the Free Corner

2.3 Vertical Compressive Stress

All three models considered in this paper omit the influence of the vertical compressive stress. In a study conducted by de Raaf et al. (2011) the influence of vertical compressive stress on the horizontal performance of unbonded FREIs was investigated. It was shown that the effective horizontal stiffness has a negative correlation with the vertical compressive stress. To date, no solution relating the vertical compressive stress to the shear behaviour for unbonded FREIs exists. The problem is complicated by the roll-over of the isolator that simultaneously reduces the loaded area and substantially deforms the layers of elastomer and reinforcement. The complexity is further increased when full roll-over occurs. At full roll-over, the initially vertical faces of the isolator contact the upper and lower supports, applying a vertical stress to the faces. This will alter the pressure distribution and result in a sudden increase in the loaded area of the isolator.

3. Model Comparison

3.1 Shear Behaviour

The three models described above are compared against unbonded FREI experimental results from a previous study. The experimental results considered are the average of seven isolators from Foster (2011). The thickness of the two exterior layers of elastomer was half the thickness of the five interior layers. The material and geometric properties of the FREI, MC1, for an interior layer are listed in Table 1. In the experimental program each isolator was subjected to three sinusoidal cycles at seven different amplitudes ranging from 0.25 t_r to 2.50 t_r at a constant average vertical stress of 2 MPa.

Table 1: Isolator Properties

Isolator	Material Properties			Geometric Properties					
	G_e (MPa)	E_e (MPa)	E_f (MPa)	2b (mm)	2a (mm)	t_e (mm)	t_r (mm)	t_f (mm)	h (mm)
MC1	0.35	1.05	20,000	63	63	3.18	19.05	0.55	22.35

Figure 7 shows the normalized experimental results with 15 % error bars from the first cycles. Since the models differ from each other based on the amount of roll-over, there is negligible difference between each model at lower horizontal displacement. As the horizontal displacement increases, the

discrepancies between each model begin to increase significantly. Model 1 provides a lower bound solution representing the central section of the isolator. The difference between Model 1 and Model 2 or Model 3 is due to the contribution of the roll-over sections of the respective model. Although Model 1 is able to accurately capture the behaviour at low and intermediate displacements, instability is incorrectly predicted at a horizontal displacement of 1.65 t_r. The prediction of instability neglects the significant advantages associated with full roll-over and the stiffening of the isolator at higher displacement amplitudes. It should be noted that Model 1 is not intended to predict the performance of the isolator past the point of instability and is continued past full roll-over in Figure 7 for comparative purposes.

Model 2 is able to capture the characteristic softening of the isolator, but overall it significantly over predicts the stiffness of the isolator. The over prediction is contributed to the selection of the elastic modulus of the fiber reinforcement. The prediction of the horizontal displacement at full roll-over provided by Model 3 is 1.86 t_r. This value agrees well with the observed horizontal displacement at full roll-over in the experimental study. A notable change in tangential stiffness in Model 3 occurs after full roll-over representing the change in boundary conditions of the isolator. During intermediate displacements, 1.00 t_r to 2.00 t_r, the model over predicts the experimental results.

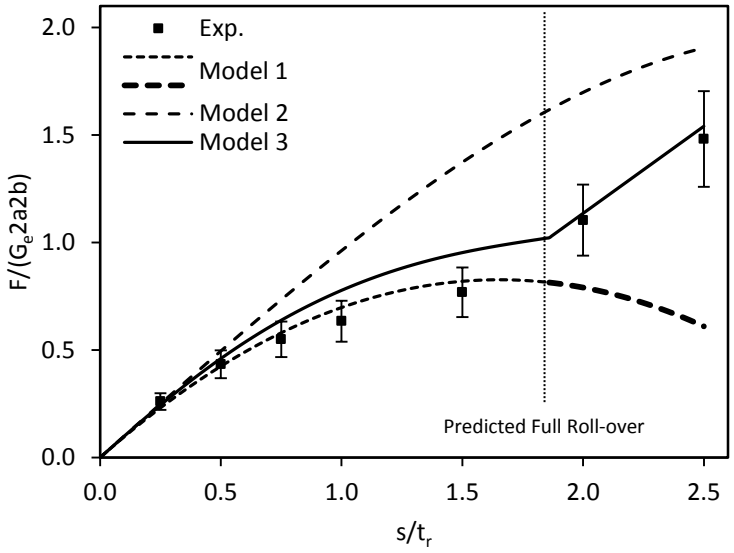

Figure 7: Model Comparison for MC1

3.2 Force Contribution

The force contribution from the central section and the roll-over sections is shown in Figure 8. As described above, initially the roll-over sections contribution to the total horizontal force is small, accounting for about 5 % of the total horizontal force at 0.25 t_r. As the horizontal displacement increases the contribution of the roll-over sections becomes more significant, accounting for 10 % and 20 % of the total horizontal force at 1.00 t_r and 1.86 t_r, respectively. It should be noted that the central section is adjusted for full roll-over in Model 3 and a notable change in tangential stiffness is observed from the central section. Similarly, the contribution from the roll-over sections has an increase in the tangential stiffness at full roll-over. At 2.50 t_r, the maximum considered horizontal displacement, the roll-over sections account for 29 % of the total horizontal force. Observing the contribution of the roll-over sections it can be seen that a significant portion of the response can be attributed to the roll-over sections and should be included in analysis.

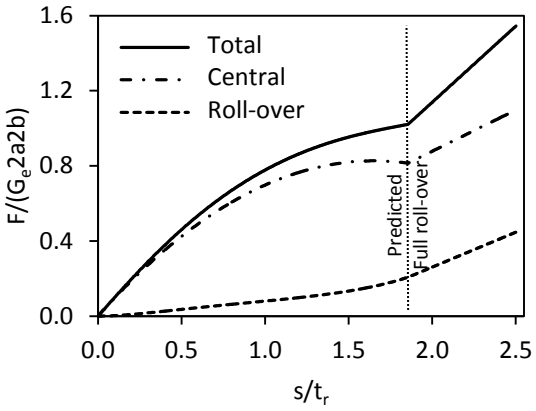

Figure 8: Central and Roll-over Sections Force Contribution

4. Modified End and Support Geometry

Tait et al. (2008) introduced the concept of modifying the end geometry of unbonded FREIs. An experimental study was conducted on four unbonded FREI specimens. The study compared the effective horizontal stiffness, k_h, and equivalent viscous damping, ζ, of the isolators obtained through horizontal cyclic testing. Three of the designs considered are shown in Figure 9. Removing material was found to decrease the effective horizontal stiffness, but to a larger degree for RB3 at displacements between 0.25 t_r and 1.00 t_r as illustrated in Figure 10a. The equivalent viscous damping was shown to be heavily influenced by the end geometry at 0.25 t_r but to a lesser degree as the displacement increased up to 1.50 t_r for RB3 as illustrated in Figure 10b.

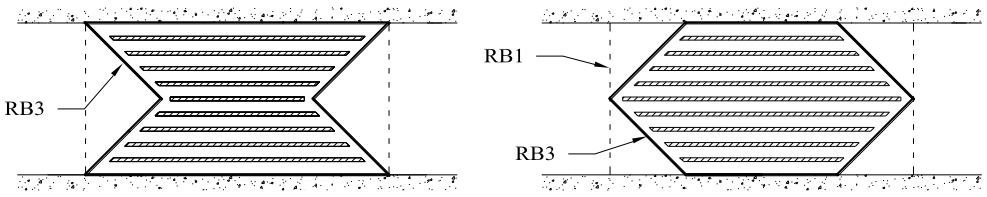

Figure 9: FREIs with Modified End Geometry

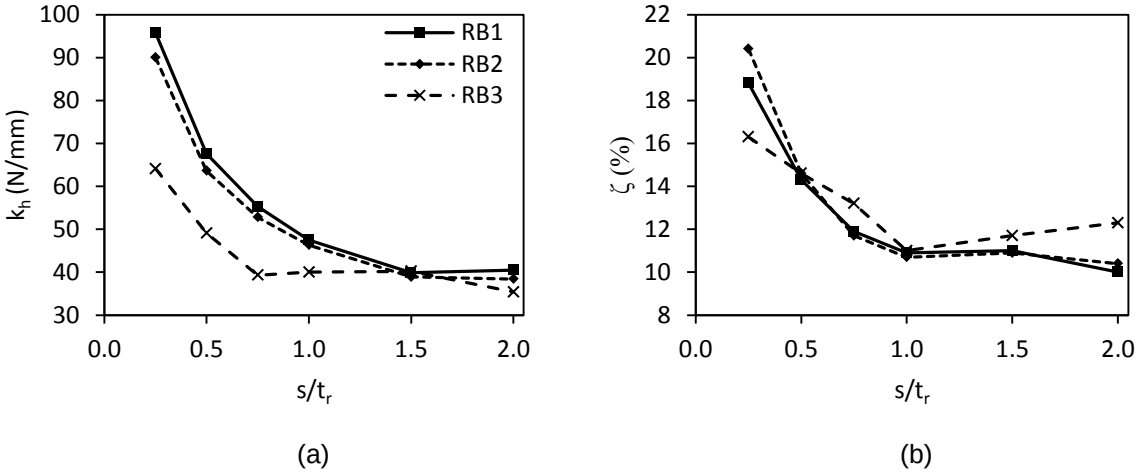

Figure 10: Selected Tait et al. (2008) findings for (a) k_h and (b) ζ as a function of s/t_r

Tait et al. (2008) also introduced the concept of modifying the support geometry, thus either accelerating or delaying full roll-over. Unlike modified end geometry, Modified Support Geometry (MSG) has no influence over the isolator response prior to full roll-over and serves only to accelerate or delay the occurrence of full roll-over. MSG may also influence the full roll-over stiffening behaviour.

Model 3 can be readily adapted to consider MSG by adjusting the condition for full roll-over. Figure 11a shows a MSG that will accelerate full roll-over by reducing the contact height, h_c. Figure 12a shows the effect of reducing the contact height for a range of h_c = 0.5 h to 1.0 h for MC1. A reduced contact height of h_c = 0.5 h represents the theoretical maximum reduction in order to avoid impact of the upper and lower supports, while h_c = 1.0 h represents unmodified geometry. It can be seen that decreasing the contact height accelerates full roll-over, stiffening the response at a lower horizontal displacement. At h_c = 1.0 h full roll-over occurred at 1.86 t_r. For h_c = 0.9 h, this was reduced to 1.74 t_r and as low as 1.25 t_r for h_c = 0.5 h. For MC1, the horizontal displacement at full roll-over can be reduced by a maximum of 33 % compared to full roll-over for h_c = 1.0 h.

An example of a MSG that will delay full roll-over is illustrated in Figure 11b. The influence of the contact height over the range of h_c = 1.0 h to 1.5 h is shown in Figure 12b for MC1. Theoretically, according to Model 3, no limit on the maximum contact height exists, although in reality the isolator would be subject to material and situation constraints. The range considered in this study was selected to observe full roll-over within the maximum considered displacement of 2.50 t_r. Horizontal displacement at full roll-over was increased from 1.86 t_r to 1.97 t_r for h_c = 1.1 h. Horizontal displacement at full roll-over was as high as 2.43 t_r for h_c = 1.5 h. For MC1, the displacement at full roll-over was increased by a maximum of 31 %.

It is important to note that despite delaying full roll-over to 2.44 t_r by increasing the contact height to 1.5 h that the tangential stiffness remains positive throughout all levels of imposed displacement, maintaining stability. This suggests that the softening range of the isolator can be significantly increased and a lower effective horizontal stiffness can be obtained without compromising the stability of the isolator. In contrast, Model 1, which does not account for MSG, predicts instability for MC1 at 1.65 t_r which could potentially overlook 32 % of the softening range of the isolator prior to full roll-over, a valuable characteristic in unbonded FREI design. This also further demonstrates the importance of including the contributions of the roll-over sections.

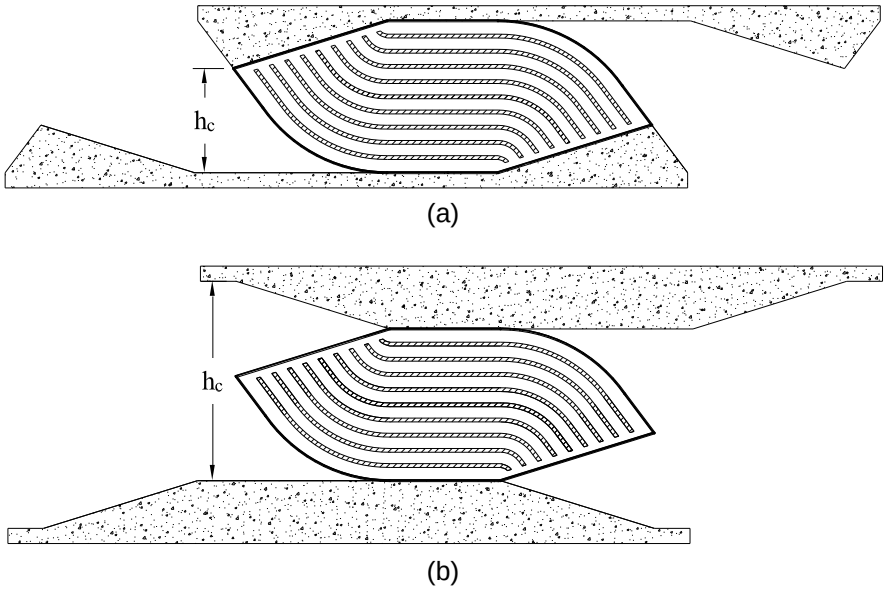

Figure 11: Unbonded FREI with Modified Support Geometry (a) Accelerating and (b) Delaying Full roll-over

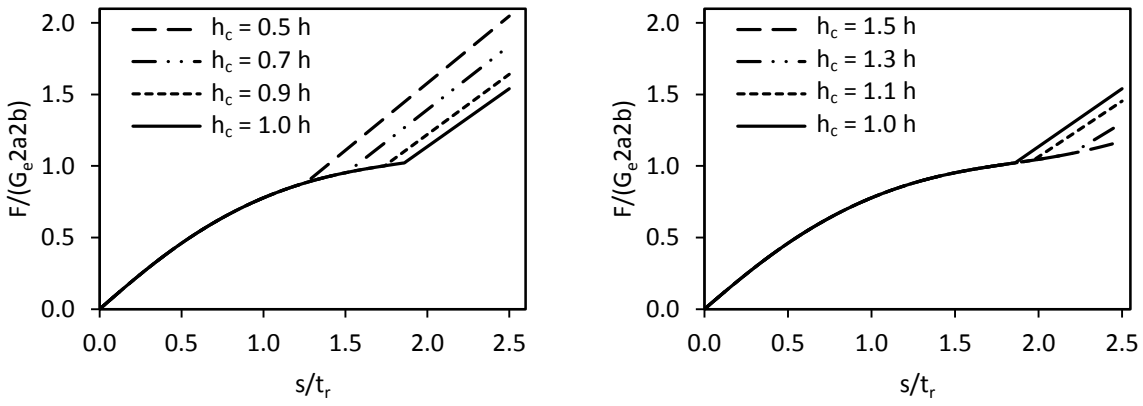

Figure 12: Influence of (a) Accelerated and (b) delayed Full roll-over for MC1

The horizontal displacement at full roll-over for the range of h_c considered is shown in Table 2. It is interesting to note that despite the non-linear nature of the model that the relationship between h_c and s at full roll-over is approximately linear. A 10 % increase in h_c results in a 6 % or 7 % increase in the horizontal displacement at full roll-over with respect to s at h_c = 1.0 h. For example, increasing h_c from 1.1 h to 1.2 h increases the horizontal displacement at full roll-over by 6 % from 106 % of h_c = 1.0 h to 112 % of h_c = 1.0 h.

Table 2: Horizontal Displacement at Full roll-over for Different Values of h_c

Full roll-over	h_c (h)										
	0.5	0.6	0.7	0.8	0.9	1.0	1.1	1.2	1.3	1.4	1.5
s/t_r	1.25	1.38	1.50	1.62	1.74	1.86	1.97	2.09	2.20	2.32	2.43
s/t_r (% of h_c = h)	67	74	81	87	94	100	106	112	119	125	131

5. Conclusions

This paper reviewed three analytical models used to determine the shear behaviour of unbonded FREIs. The models were compared against the experimental results from an earlier study on seven unbonded FREIs. Model 1 provided a lower-bound solution based on the assumption that the roll-over sections are completely stress free. This model was shown to provide an acceptable prediction up to intermediate horizontal displacements when the model may inappropriately predict instability. Omitting the roll-over section neglects the significant advantages associated with unbonded FREIs at high horizontal displacements but offers a simple approach to modelling lower horizontal displacements.

Model 2 and Model 3 are similar but differ notably on the assumed relationship between the horizontal displacement and the bending displacement of the roll-over sections. Model 2 is able to demonstrate softening but over predicts the shear force in comparison to the experimental data. Model 3 gives an indication of the deformed shape of the roll-over, predicts full roll-over, and the full roll-over performance providing an improved prediction form either Model 1 or Model 2 when compared to the experimental data.

Unbonded FREIs can be modified through alterations to the end or support geometry to optimize their performance. From Model 3, it was shown that full roll-over can be accelerated or delayed by modifying the contact height. It was demonstrated that full roll-over could occur over a range of 1.26 t_r to 2.44 t_r representing about a ±30 % range compared to an unbonded FREI with unmodified support geometry. If full roll-over is delayed, the isolator will continue to soften, increasing the overall efficiency of the isolation

system. The isolator considered remained stable despite a significant delay in full roll-over, further reinforcing that the contribution of the roll-over sections is important and should not be ignored. Experimental testing is required to verify the favourable results obtained from Model 3, specifically the full roll-over behaviour for FREIs with modified support geometry.

The influence of vertical compressive stress on the horizontal properties of the isolator is notably missing from all three models considered. This is an important parameter and is an ideal next step in the development of a comprehensive model for the shear relationship of unbonded FREIs.

Acknowledgements

This research was carried out as part of the mandate of the McMaster University Centre for Effective Design of Structures and funded through the Natural Sciences and Engineering Research Council of Canada (NSERC).

References

de Raaf, M.G.P., Tait, M. J. and Toopchi-Nezhad, H. 2011. Stability of Fiber-reinforced Elastomeric Bearings in an Unbonded Application. *Journal of Composite Materials,* 45(18): 1873-1884.

Foster, B.A.D. 2011. Base isolation using Stable Unbonded Fibre Reinforced Elastomeric Isolators (SU-FREI), Thesis, McMaster University.

Kelly, J.M. 1999. Analysis of Fiber-reinforced Elastomeric Isolators. *Journal of Seismology and Earthquake Engineering,* 2(1): 19-34.

Kelly J.M. and Konstantinidis, D. 2007. Low-cost Seismic Isolators for Housing in Highly-seismic Developing Countries. *10th World Conference on Seismic Isolation, Energy Dissipation and Active Vibrations Control of Structures,* Istanbul, Turkey.

Kelly, J.M. and Konstantinidis, D. 2011. *Mechanics of Rubber Bearings for Seismic Isolation and Vibration Isolation*, John Wiley & Sons, Chichester, UK.

Kelly, J.M. and Marsico, M.R. 2010. Stability and Post-Buckling Behavior in Nonbolted Elastomeric Isolators. *Seismic Isolation and Protection Systems*, 1:41-54.

Konstantinidis, D., Kelly, J.M. and Makris, N. 2008. Experimental Investigations on the Seismic Response of Bridge Bearings. Earthquake Engineering Research Center: University of California, Berkeley; Report EERC 2008-02.

Moon B.Y., Kang G.J., Kang, B.S. and Kelly, J.M. 2002. Design and Manufacturing of Fiber Reinforced Elastomeric Isolator for Seismic Isolation. *Journal of Materials Processing Technology*, 130-131:145-150.

Peng, T.B., Zhang, H., Li, J.Z. and Li, W.X. 2009. Pilot Study on the Horizontal Shear Behaviour of FRP Rubber Isolators. *Journal of Vibration and Shock*, 28:127-130. [in Chinese]

Swiss Re. 2012. Lessons from Recent Major Earthquakes. Available: www.swissre.com.

Taghavi, S. and Miranda, E. 2003. Response Assessment of Nonstructural Building Elements. Pacific Earthquake Engineering Research Center: Stanford University; Report 2003/05.

Tait, M.J., Toopchi-Nezhad, H. and Drysdale, R.G. 2008. Influence of End Geometry on Fiber Reinforced Elastomeric Isolator Bearings. *14th World Conference on Earthquake Engineering,* Beijing China.

Toopchi-Nezhad, H., Tait, M.J. and Drysdale, R.G. 2008. Testing and Modeling of Square Carbon Fiber-reinforced Elastomeric Seismic Isolators. *Structural Control and Health Monitoring*, 15: 876-900.